



Sorption of CO₂/CH₄ mixtures in TZ-PIM, PIM-1 and PTMSP: Experimental data and NELF-model analysis of competitive sorption and selectivity in mixed gases



Eleonora Ricci^{a,*}, Aweke Elias Gemedo^a, Naiying Du^b, Nanwen Li^c, Maria Grazia De Angelis^a, Michael D. Guiver^{d,e}, Giulio C. Sarti^a

^a Dipartimento di Ingegneria Civile, Chimica, Ambientale e dei Materiali (DICAM), Università di Bologna, Via Terracini 28, 40131 Bologna, Italy

^b National Research Council Canada, 1200 Montreal Road, Ottawa, Ontario, K1A 0R6, Canada

^c State Key Laboratory of Coal Conversion, Institute of Coal Chemistry, Chinese Academy of Sciences, Taiyuan, 030001, China

^d State Key Laboratory of Engines, School of Mechanical Engineering, Tianjin University, Tianjin 300072, China

^e Collaborative Innovation Center of Chemical Science and Engineering (Tianjin), Tianjin 300072, China

ARTICLE INFO

Keywords:

Gas separation
Mixed-gas sorption
PIMs
Glassy polymers
NELF model

ABSTRACT

The sorption of CO₂, CH₄ and CO₂/CH₄ mixtures in poly(trimethylsilyl propyne) (PTMSP) and PIM-1 (the first reported polymer of intrinsic microporosity) measured in previous works revealed that, in the multicomponent case, significant exclusion effects cause a decrease in solubility with respect to the pure-gas case, and this effect is more pronounced for the less soluble gas (CH₄). In this work we perform a similar experimental analysis on the tetrazole-modified PIM-1 (TZ-PIM), at three mixture compositions (10, 30, 50 mol.% CO₂) and three temperatures (25, 35, 50 °C), up to 35 bar. The obtained trends for solubility and solubility-selectivity of CO₂, CH₄, and their mixtures in TZ-PIM are found to be qualitatively and quantitatively comparable to those obtained for other high free volume polymers. Moreover, mixed-gas sorption data collected so far for three materials (TZ-PIM, PIM-1 and PTMSP) are modelled by means of the Non-Equilibrium Lattice Fluid (NELF) model and compared with experimental results. The model was found capable of representing the competitive effects in solubility and solubility-selectivity, in a wide range of temperature and pressure, with a better quantitative accuracy attained at higher temperatures. Finally, by coupling these results with mixed-gas permeation data, an estimate of the mixed-gas diffusivity was obtained, and it was revealed that, in multicomponent conditions, sorption provides a greater contribution to the selectivity than diffusivity, in agreement with experimental findings for similar materials.

1. Introduction

Polymers are used as membrane materials in several industrial, medical and environmental applications dealing with separation and purification of gases and liquids, including desalination, dialysis, food processing and packaging, sensor development, and gas separation. Nowadays, gas separation with membranes is employed industrially for hydrogen recovery, nitrogen production, air dehydration, and natural gas sweetening [1–4]. However, in order to promote a larger market penetration of this gas separation technology, better membranes are needed. One of the challenges posed by the use of polymeric materials as membranes is that they are subject to a trade-off between permeability and selectivity: for every gas pair the log of selectivity versus the log of the permeability of the most permeable gas has been shown to lie

at or below a limiting line, customarily referred to as the Robeson upper bound [5,6]. Ultra-permeable materials usually lack in selectivity, whereas highly-selective materials exhibit lower permeability [6]. Therefore, the efficiency that can be achieved by the operation in terms of purity and productivity is limited and it is always necessary to find the right compromise between these factors [7,8] in order to maximize the process economy.

In recent years, innovative materials with improved performance, capable of surpassing the 2008 upper bound [6] for several gas couples, have been developed [9–13]. A major breakthrough in membrane materials research was witnessed with the new class of Polymers of Intrinsic Microporosity (PIMs) [14–21]. These materials have shown very high gas permeation rates, while maintaining acceptable selectivity values, and moreover they provide good thermal and chemical

* Corresponding author.

E-mail address: eleonora.ricci12@unibo.it (E. Ricci).

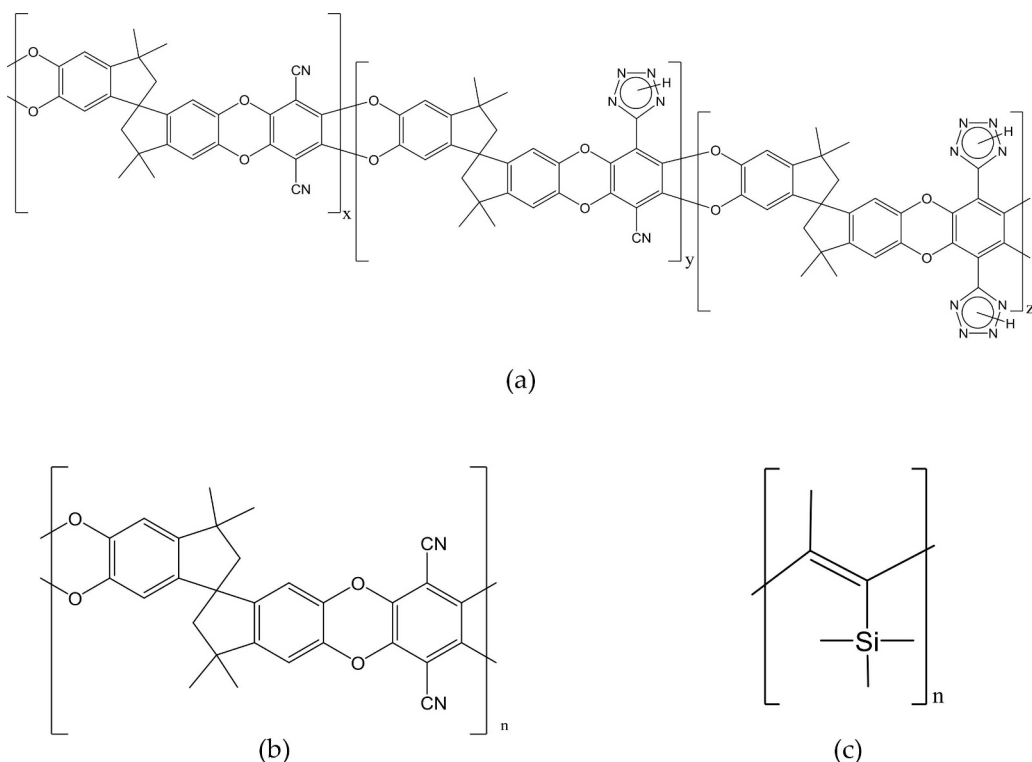


Fig. 1. (a) Repeating unit of the polymer considered in this study: TZ-PIM. (b) Repeating unit of PIM-1 (TZ-PIM precursor). (c) Repeating unit of PTMSP, considered as a benchmark material.

stability [17]. The ladder-like backbone of these polymers consists of condensed rings and is therefore severely rotationally hindered. Moreover, the presence of contortion sites in the repeating unit results in exceptionally high free volume, organized as a network of regular interconnected micro-cavities, capable of sieving effects, as shown by experimental and molecular simulation investigations [22–28].

In this study TZ-PIM, a PIM functionalized with CO₂-philic pendant tetrazole groups, is considered. TZ-PIM constitutes an attempt at improving the selectivity of PIM-1 towards CO₂ by incorporating groups that are more CO₂-philic into its structure. In particular, the nitrile groups of PIM-1 were substituted with tetrazole groups, demonstrating that post-polymerization modification techniques with controlled conversion rates represent a viable way of tuning the separation properties of these innovative materials. The structures of TZ-PIM and PIM-1 can be compared in Fig. 1.

Using nuclear magnetic resonance (NMR) spectroscopy, it was demonstrated that the CO₂ molecules interact with tetrazole sites through physisorption [29] and the presence of these strongly CO₂-sorbing groups in a highly porous polymeric matrix has been proven capable of increasing the selectivity, without compromising the permeability excessively, leading to an overall performance which lies beyond the 2008 upper bound. Here, the mixed-gas CO₂/CH₄ sorption behaviour of TZ-PIM was measured and compared with that of its precursor material, PIM-1, in order to assess the effect of the functionalization in multicomponent conditions.

The relevance of mixed-gas tests lies in the necessity to characterize the relevant material properties, namely its permeability and selectivity, as close as possible to the actual operating conditions, due to the non-idealities that are present in the actual multicomponent case. At present, the characterization of membrane materials is often performed with pure gases only and fewer data exist in the literature for the mixed-gas performance of polymeric membranes. While the pure-gas measurements are a necessary first step in the characterization of a material, they are very often a poor predictor of the performance in actual operating conditions [30], since the multicomponent behaviour

can deviate significantly from the permeability and selectivity values estimated based on pure-gas data alone [17,31–34].

In particular, in the case of sorption in glassy polymers, great non-idealities are present, due to competition between the sorbing gases, which lowers their solubility with respect to the pure-gas case.

Experimentally, mixed-gas tests are delicate and much more time-consuming than pure-gas tests, so there is a potential advantage in the use of reliable modelling tools capable of predicting the mixed-gas behaviour using pure-gas experimental information only. In this work we address this issue by applying a thermodynamics-based model to the prediction of mixed-gas sorption in glassy polymers.

The transport of small molecules in dense polymeric membranes is described by the solution-diffusion model [35], according to which permeability (P) is the product of the solubility (S) and diffusion coefficients (D):

$$P = S \cdot D \quad (1)$$

Consequently, the selectivity of the polymer, which is equal to the ratio between the permeabilities of the two gases, when the downstream pressure is negligibly small becomes the product of a solubility-selectivity and a diffusivity-selectivity factor:

$$\alpha_{i,j} = \frac{P_i}{P_j} = \frac{S_i}{S_j} \cdot \frac{D_i}{D_j} = \alpha_{i,j}^S \cdot \alpha_{i,j}^D \quad (2)$$

The calculation of gas solubility in polymeric systems is customarily performed in the literature using the Dual Mode (DM) sorption model [36–43]. This model divides the total sorbed gas into two contributions: the molecules dissolving into the dense portion of the polymer (following Henry's law), and those saturating the microvoids of the excess free volume that characterizes the glassy state (described by a Langmuir curve). Despite some limitations inherent to its empirical nature, it is frequently employed, thanks to its simplicity of use and its capability to correlate the experimental sorption behaviour in glassy polymers very well in most cases, even if not always. The model can be straightforwardly extended to the multicomponent case [44] and allows predictive

calculation of mixed-gas sorption isotherms, once pure component parameters have been best fitted to the pure component sorption isotherms. The accuracy of mixed-gas sorption isotherms calculation with the Dual Mode model was assessed in a separate work [45], with the finding that the model correctly displays the qualitative behaviour of the system under consideration, but the quantitative agreement with experimental data is less satisfactory.

The calculation of gas sorption equilibria can be performed with Equations of State (EoS) models, such as those based on a Lattice Fluid (LF) representation of substances [46], or on hard sphere chain schemes, like the Statistical Associating Fluid Theory (SAFT) [47], suitably extended to the nonequilibrium conditions of the glassy phases. An extension to the nonequilibrium state of glassy polymers is provided by the Non-Equilibrium Thermodynamics for Glassy Polymers (NET-GP) approach [48], that gives nonequilibrium expressions for the above mentioned EoS, by introducing an internal state variable, the polymer density, to describe the out-of-equilibrium degree of the systems. This model has been successfully applied to the prediction of gas and vapor sorption in a variety of polymeric systems [49–52] and it will be further described in the following section.

It is also possible to use atomistic simulations for the prediction of sorption isotherms, for example with Monte Carlo simulations in the Grand Canonical ensemble [53] or in the NPT-Gibbs Ensemble [54]. Alternatively, gas solubility can be extracted from the post-processing of Molecular Dynamics (MD) or Monte Carlo (MC) trajectories, using the Widom Particle Insertion method [55] or the Staged Particle Deletion [56] and Direct Particle Deletion [57] schemes. In recent years, the properties of microporous polymers for membrane applications have been extensively investigated with atomistic simulation techniques [18,26,58–60]. Sorption of CO₂ in PIM-1 was first simulated by Heuchel et al. [61] employing the Gusev-Suter transition state theory [62,63], which yielded solubility coefficients that were systematically higher than the experimental ones. Fang et al. [64,65] applied the Widom Insertion method instead, and their results for CO₂ solubility in PIM-1 are in close agreement with the experimental ones. Recently, Kupgan et al. [66] simulated CO₂ sorption in PIM-1 up to 50 bar, employing a scheme combining Grand Canonical Monte Carlo and Molecular Dynamics simulations [67]. Frentrup et al. [68] performed Nonequilibrium Molecular Dynamics simulations for the direct simulation of He and CO₂ permeability through a thin membrane of PIM-1, which was in good qualitative agreement with experimental data. As the ever increasing computational power allows for more accurate potentials to be developed and longer simulations to be run, the reliability of the predictions made by atomistic techniques has improved accordingly [69]. However, the extremely high computational effort required by these approaches remains a major drawback to the application of such techniques to the study of the gas separation properties of polymers, especially in the glassy state.

Fewer modelling and simulation studies deal with the analysis of mixed-gas sorption effects. Recently Rizzuto et al. [70] have studied the mixed-gas permeation properties of CO₂/N₂ mixtures in Thermally-Rearranged polymers combining Grand Canonical Monte Carlo atomistic simulations and Ideal Adsorbed Solution Theory (IAST) [71]. Pure-gas sorption of both gases was underestimated by the simulations. However, the competitive effects between the components in the mixture, expected in the case of glassy polymers, were displayed and found to affect greatly the solubility of the less condensable gas of the mixture. Neyertz and Brown [72] performed large-scale MD simulations of air separation with an ultra-thin polyimide membrane surrounded by an explicit gas reservoir. In their work, gas solubility, diffusivity and O₂/N₂ selectivity were determined predictively in multicomponent conditions and compared favourably with experimental results. Similarly, Tanis et al. [73] studied CH₄/N₂ separation with several polyimide membranes using atomistic simulations. They combined solubility coefficients obtained from excluded-volume map sampling test-particle insertions and diffusion coefficients calculated with a variant of

the kinetic Monte Carlo approach. Iterative procedures allowed to account for swelling effects upon sorption, both in the pure- and in the mixed-gas case. Their results highlighted non-ideal behaviour in the multicomponent case, affecting both the predicted permeability and selectivity of the membrane material.

In this work, gas solubility, both in pure- and mixed-gas conditions, was modelled using the NELF model [74]. The modelling analysis was performed to study the data measured in this work for CO₂/CH₄ sorption in TZ-PIM. In addition, the modelling analysis was performed also on PIM-1 and PTMSP [31–33], some of the few materials for which the multicomponent sorption behaviour of CO₂/CH₄ mixtures has been characterized experimentally, but for which no modelling of these properties was reported previously.

2. Experimental

2.1. Membrane film formation

TZ-PIM was obtained through post-polymerization modifications of PIM-1, as described in Ref. [75]. Depending on the reaction time, the conversion of nitrile groups of PIM-1 to tetrazole groups can range from 50 to 100%. The material used in this study had a conversion of about 55% and is referred to as TZ-PIM-1 [75].

Gases for sorption tests were purchased from SIAD and used without further purification. Dense polymer films of TZ-PIM for gas sorption measurements were prepared from slow evaporation of 2 wt% solutions in dimethylacetamide. After several washes in water, the membranes were soaked in methanol for 24 h to remove residual solvent and then dried in a vacuum oven at 120 °C for 24 h. The density of the film was measured by the buoyancy technique [76], using heptane as a displacement fluid, obtaining a value of 1.186 g/cm³ at room temperature.

2.2. Pure- and mixed-gas sorption measurements

Sorption experiments were performed using a pressure decay apparatus, whose design is an elaborate evolution of that used by Sanders et al. [77] and which has been described in detail in previous works [31,32]. To perform mixed-gas sorption tests, the apparatus is equipped with a gas chromatograph Varian CP4900 Micro-GC with a capillary column PoraPLOT U and thermal conductivity detector. The apparatus is submerged in a thermostatted recirculated water bath.

The details of the measurement protocol adopted for pure- and mixed-gas tests with this apparatus were optimized to maximize the flexibility of the equipment and are reported in detail elsewhere [31]. Before each test, the samples were kept under vacuum overnight at the temperature of the experiment, in order to ensure that any residual gaseous or vapor components were evacuated. Pure-gas tests were performed differentially, by increasing the gas pressure after each equilibration step, without evacuating the system, whereas in mixed-gas tests, vacuum was pulled after each equilibration step (integral experiment).

Tests were performed for pure CO₂ and pure CH₄ sorption in TZ-PIM at 25, 35, 50 °C and for three CO₂/CH₄ mixtures (10, 30, 50 mol.% CO₂) at the same three temperatures, up to 35 bar of total pressure.

3. Theoretical background

3.1. NET-GP theory

The Non-Equilibrium Thermodynamics for Glassy Polymers (NET-GP) approach [48,50,74] is a thermodynamics-based framework which provides an extension of Equation of State (EoS) theories to nonequilibrium materials, and is therefore suitable for the calculation of the solubility of low molecular weight species in glassy polymers, which could not be described correctly by equilibrium equations of state or activity coefficients models, due to the nonequilibrium nature of such

materials. The NET-GP approach applies to homogeneous, isotropic, and amorphous phases, whose state is described by the usual set of state variables, namely temperature, pressure and composition, and, in addition, by the actual nonequilibrium density of the glassy polymer ρ_{pol} which acts as an internal state variable and accounts for all the effects of thermal history and formation of the polymer, responsible for its departure from equilibrium. The Helmholtz free energy density a^{NE} of a polymer-penetrant system with an internal state variable is given by Equation (3):

$$a^{NE} = a^{NE}(T, p, \Omega, \rho_{pol}) \quad (3)$$

in which the composition vector, Ω , contains the mass ratios between the i th penetrant and the polymer. It can be shown [50] that a^{NE} is independent of pressure:

$$\left(\frac{\partial a^{NE}}{\partial p} \right)_{T, \rho_i, \rho_{pol}} = 0 \quad (4)$$

The main result of the NET-GP approach is thus that the nonequilibrium Helmholtz free energy of the system can be related to a corresponding equilibrium value a^{Eq} , at the same temperature, density and composition:

$$a^{NE}(T, p, \Omega, \rho_{pol}) = a^{Eq}(T, \Omega, \rho_{pol}) \quad (5)$$

For the chemical potential under nonequilibrium conditions the following relation holds [50]:

$$\mu_i^{NE} = \left(\frac{\partial a^{NE}}{\partial \rho_i} \right)_{T, \rho_j \neq i, \rho_{pol}} \quad (6)$$

As a consequence, the nonequilibrium chemical potential can be obtained from the corresponding equilibrium value at the same temperature, density and composition:

$$\mu_i^{NE}(T, p, \Omega, \rho_{pol}) = \mu_i^{Eq}(T, \Omega, \rho_{pol}) \quad (7)$$

Therefore, it is possible to calculate the chemical potential in nonequilibrium conditions using the expression for the free energy provided by an EoS of choice and employ it to solve the phase equilibrium for the composition:

$$\mu_i^{NE(pol)}(T, p, \Omega, \rho_{pol}) = \mu_i^{Eq(gas)}(T, p, y_i) \quad (8)$$

The equilibrium chemical potential in the gas phase $\mu_i^{Eq(gas)}$ is obtained by means of a suitable equation of state for the gas phase.

The NET-GP approach requires knowledge of the polymer density at each pressure value used in the computation of the sorption isotherm. For the proper evaluation of its value during sorption, experimental dilation measurements would be needed, because the presence of swelling agents can significantly alter it, especially at high pressure. However, with the lack of such data, a linear relation between the polymer specific volume and the partial pressure of the penetrant can be assumed, as it has often been observed experimentally for different light gases [78–80]. In these conditions, adjustable swelling coefficients $k_{sw,i}$ can be defined as follows (Eq. (9)):

$$\frac{1}{\rho_{pol}} = \frac{1}{\rho_{pol}^0} \left(1 + \sum_{i=1}^{N_p} k_{sw,i} p_i \right) \quad (9)$$

In the case of a single penetrant, k_{sw} can be evaluated by the knowledge of one point of the sorption isotherm in the high-pressure range. When T_g is experimentally accessible, k_{sw} values can also be estimated in a predictive way by using the rheology model presented in Ref. [49].

3.2. NELF model

Sorption equilibria in the glassy polymer phases considered will be

calculated hereafter by using the NELF model [48,50,74,81], which is the extension of the Sanchez-Lacombe (SL) EoS [46,82,83] to the nonequilibrium glassy state by means of the NET-GP theory. In the lattice fluid representation, matter is seen as a lattice, whose cells can be empty or occupied by molecular segments. The characteristic pure component parameters finally used are: the molar volume of a lattice cell of component i (v_i^*), the number of lattice cells occupied by molecule of component i (r_i) and the non-bonded interaction energy between two cells occupied by component i (ε_i^*). Alternatively, the characteristic temperature (T_i^*), characteristic pressure (p_i^*) and characteristic density (ρ_i^*) can be used. Mixture properties are described by using the pure component parameters of each species in addition to the binary interaction parameters k_{ij} entering the model mixing rules. The relationships among the materials parameters along with the relevant expressions and mixing rules are reported in the Supplementary Information file, in Table S1.

In the nonequilibrium case, the polymer density value, that is needed to calculate the parameters, has to be known experimentally. In the case of the gas phase, the equilibrium density results from the solution of the SL EoS (Eq. (10)), which is formally identical for pure components and mixtures, provided that the corresponding definition (i.e. that for a pure component or that for the multicomponent case) of the reduced variables \tilde{T} , \tilde{p} , $\tilde{\rho}$ is used.

$$\tilde{\rho} = 1 - \exp \left[-\frac{\tilde{\rho}^2}{\tilde{T}} - \frac{\tilde{p}}{\tilde{T}} - \tilde{\rho} \left(1 - \sum_i^N \frac{\phi_i}{r_i} \right) \right] \quad (10)$$

The expression of the chemical potential of the SL model, to be used in Eq. (8), is given below.

$$\frac{\mu_i}{RT} = \ln(\tilde{\rho}\phi_i) - \ln(1 - \tilde{\rho}) \left[r_i^0 + \frac{r_i + r_i^0}{\tilde{\rho}} \right] - r_i - \tilde{\rho} \frac{r_i^0 v_i^*}{RT} \left[p_i^* + \sum_{j=1}^N \phi_j \left(p_j^* - \Delta p_{i,j}^* \right) \right] + 1 \quad (11)$$

Definitions of the variables used in Eq. (10) and Eq. (11) are reported in Table S1.

3.3. Mixed-gas sorption calculation

The first step of the calculation consists of the analysis of pure-gas sorption isotherms with the model, in order to obtain the values of the binary interaction parameter k_{ij} and the swelling coefficient k_{sw} . The binary interaction parameter is obtained from the best fit of the low-pressure range of the sorption isotherms, taking advantage of the fact that, in these conditions, penetrant-induced swelling is negligible, and therefore the value of k_{sw} does not influence the result and can be set equal to zero. The final value of k_{sw} is subsequently obtained from the best fit of the high-pressure range of the curve, once the appropriate value for k_{ij} has been retrieved. These parameters are then used to evaluate sorption in mixed-gas conditions, solving the phase equilibrium equations (Eq. (8)). Even in the multicomponent case, only binary interactions are considered, according to the mixing rule of the lattice fluid theory; the k_{ij} values for the interactions between the penetrant species are set equal to zero [52], in view of their high dilution in the polymer mixture.

Finally, the results of the calculations are used to evaluate the solubility-selectivity. The solubility-selectivity can be calculated both for pure-gas sorption (ideal case) and for multicomponent sorption (real case) making use of the definition of the solubility coefficient S :

$$\alpha_{CO_2, CH_4}^S = \frac{S_{CO_2}}{S_{CH_4}} = \frac{c_{CO_2}/f_{CO_2}}{c_{CH_4}/f_{CH_4}} \quad (12)$$

using the corresponding value of the gas concentrations c , in pure- or mixed-gas conditions. Gas fugacities (f_i) at the various pressures were calculated with the Peng-Robinson equation of state [84], both in pure-

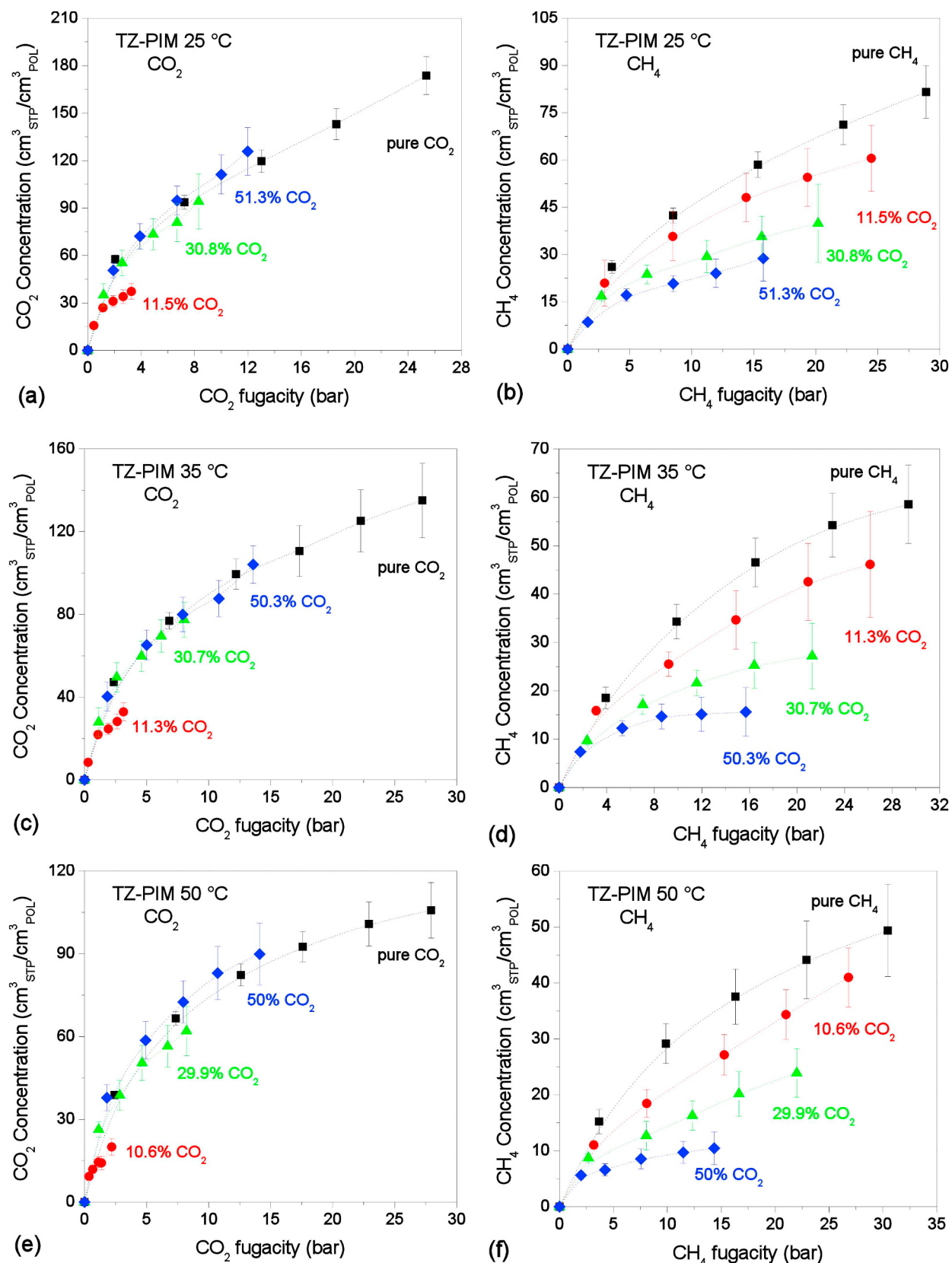


Fig. 2. Sorption isotherms of CO_2 (a,c,e) and CH_4 (b,d,f) at 25, 35, 50 °C in TZ-PIM, in pure- and mixed-gas conditions (Black squares: pure-gas; Red circles: ~10% CO_2 mixture; Green triangles: ~30% CO_2 mixture; Blue diamonds: ~50% CO_2 mixture). Lines are drawn to guide the eye. (For interpretation of the references to colour in this figure legend, the reader is referred to the Web version of this article.)

and mixed-gas conditions. For the CO_2/CH_4 mixtures in the gas phase, the binary parameter $k_{\text{CO}_2,\text{CH}_4} = 0.09$ was used [85] in the mixing rule of Peng-Robinson EoS.

4. Experimental results

4.1. Pure and mixed gas sorption isotherms in TZ-PIM

Sorption isotherms of pure CO_2 and CH_4 and three different CO_2/CH_4 mixtures in TZ-PIM at 25, 35, 50 °C are reported in Fig. 2 as a function of gas fugacity. The error bars represent 95% confidence intervals. The trends reported in Fig. 2 confirm the competitive nature of mixed-gas solubility in TZ-PIM, as it was also observed for other glassy polymers [31–33]. The solubility of each species is generally lower in the mixed-gas case, and the effect increases as pressure and mole fraction of the second gas increase.

The maximum deviation to CH_4 concentration was induced by the presence of 50 mol.% CO_2 . The concentration of CH_4 sorbed from equimolar mixtures decreased up to 49% of the pure-gas value at 25 °C. The effect was even more pronounced at higher temperatures: at 35 °C the concentration of CH_4 sorbed from equimolar mixtures decreased up to 35% of the pure-gas value, reaching a maximum decrease to 29% of the pure-gas value at 50 °C. On the other hand, CO_2 concentration in mixed-gas conditions displayed a maximum decrease to about 50% of the pure gas value at all temperatures, but this decrease was measured in presence of a much higher molar fraction of the second gas (about 90 mol.% CH_4 in the mixture). It is significant that the competitive effect has a much stronger impact on CH_4 than on CO_2 solubility, such that the effect increases the CO_2/CH_4 solubility-selectivity of the membrane with respect to the ideal case.

4.2. Comparison with other glassy polymers

In Fig. 3 pure- and mixed-gas sorption of intermediate mixture compositions at 35 °C in TZ-PIM, its precursor PIM-1 (data from Ref. [32]), and another high free volume material, PTMSP (data from Ref. [31]) are compared. The comparison is carried out both in terms of sorption and solubility-selectivity. Data are reported on the same scale, in order to highlight the differences. Film formation protocols can induce significant differences in the properties of PIM membranes [86,87]. Therefore, it is relevant to highlight that both the TZ-PIM samples used in this study and the PIM-1 samples used in the reference study [32] underwent analogous film formation histories. In particular, in both cases a 24 h methanol soaking treatment was performed, followed by drying under vacuum overnight at high temperature. In the case of PTMSP, one mixture composition is different, 20 mol% CO_2 instead of ~30%, however, as it can be observed, the experimental data showed little variation between 20 and 50% in that material, therefore the comparison is still appropriate.

The amount of gas sorbed by TZ-PIM is slightly lower than that of PIM-1 for both gases in pure conditions, probably due to TZ-PIM being a denser matrix than PIM-1, as a consequence of hydrogen bonding interactions. However, in the mixed-gas case, the amount of gas sorbed by the two materials is essentially equal, thus showing the capability of the modified material of leveraging the multicomponent exclusion effect to a greater extent than its precursor. PTMSP shows lower sorption than the PIMs for both gases, despite its higher free volume: in the case of pure CH_4 the maximum difference between PTMSP and PIM-1 is around 20%, while for pure CO_2 is about 35%. The greater difference in the case of CO_2 can be explained by the absence of CO_2 -philic groups in PTMSP, while their presence, both in PIM-1 and TZ-PIM, leads to more favourable thermodynamic equilibria in terms of sorption and solubility-selectivity. In fact, it can be observed that, except for some small differences at low pressure, the values of the ideal solubility-selectivity of the three materials are very close, and, in particular, tend to stabilize at high pressure around a constant value of 2.5 for PIM-1 and TZ-PIM,

and 2 for PTMSP. On the contrary, real solubility-selectivity in multi-component conditions shows, on average, a threefold increase compared to the ideal one, both for TZ-PIM and PIM-1, while the average increase for PTMSP is only around 50%.

These observations allow also to emphasize how different the behaviour estimated with pure-gas data is from the multicomponent one, especially in the case of TZ-PIM and PIM-1: the solubility-selectivity in the conditions inspected would be underestimated by as much as a factor 3, if mixture effects were neglected.

5. NELF modelling

5.1. Pure-gas sorption isotherms analysis

The values of Sanchez-Lacombe EoS pure-component parameters used for the calculations with the NELF model are reported in Table 1. Parameters for gases and vapours are usually retrieved fitting Vapor-Liquid Equilibrium (VLE) data, whereas for polymers, the most appropriate choice would be fitting pressure-volume-temperature (*pVT*) data above the glass transition, where the material is in a state of thermodynamic equilibrium. For high free volume glassy polymer, however, these data are usually unavailable, due to degradation phenomena occurring before the glass transition is reached. In most calorimetric experiments, PIM-1, for instance, decomposed around 350 °C without an apparent glass transition [88]. Recently, Yin et al. [89] were able to observe a glass transition for PIM-1 at 442 °C without degrading the material, by employing fast scanning calorimetry. In conventional dilatometric experiments performed to measure *pVT* data, however, such heating rates, required to avoid degradation, would be unattainable.

In such cases, an alternative approach can be followed, fitting the EoS parameters on the sorption equilibrium data directly, using the nonequilibrium model [90]. The parameters for TZ-PIM and PIM-1 used in this work were indeed retrieved using this method [51,91].

Table 2 reports the values of binary interaction parameters and swelling coefficients obtained from the analysis of pure-gas sorption data with the NELF model, as detailed in Section 3.3. They are found to follow a linear temperature dependence. In all cases the values of the swelling coefficients obtained for CH_4 are lower than those of CO_2 in the corresponding case, consistently with the experimental evidence of CO_2 being a stronger swelling agent than CH_4 .

The dry polymer density values adopted are those reported for the experimental samples in the respective works: 0.770 g/cm³ for PTMSP at 35 °C [31], 1.143 g/cm³ for PIM-1 at 25 °C [32] and 1.186 g/cm³ for TZ-PIM at 25 °C, as measured in the present work. The temperature dependence of the PIMs density was accounted for, by using the thermal expansion coefficient reported in Ref. [93] for a similar material (PIM-7): $6.4 \cdot 10^{-4} \text{ K}^{-1}$. Through atomistic simulations of the volumetric properties of PIM-1 as a function of temperature, similar values of the thermal expansion coefficients were calculated: $8.3 \cdot 10^{-4} \text{ K}^{-1}$ [94] and $2.5 \cdot 10^{-4} \text{ K}^{-1}$ [95].

5.2. Mixed-gas sorption prediction

In this section the calculation of mixed-gas sorption isotherms performed for TZ-PIM, PIM-1 and PTMSP is discussed. In Fig. 4, the experimental sorption data of CO_2/CH_4 mixtures (~10/30/50 mol.% CO_2) in TZ-PIM, PIM-1 [32] and PTMSP [31] at 35 °C, together with the results of mixed-gas sorption calculations with the NELF model are reported. In all plots, error bars indicate 95% confidence intervals of the experimental points.

It can be seen in Fig. 4 that, in the case of CO_2 , the prediction of the model is very satisfactory for PIM-1 and TZ-PIM, with average relative deviations below 5%. In the case of CH_4 the accuracy is lower in the case of TZ-PIM, where average deviations between experimental data and model results are found to be 16%, 8% and 6% going from 50.3 mol.% CO_2 in the mixture to 30.7% and 11.3%.

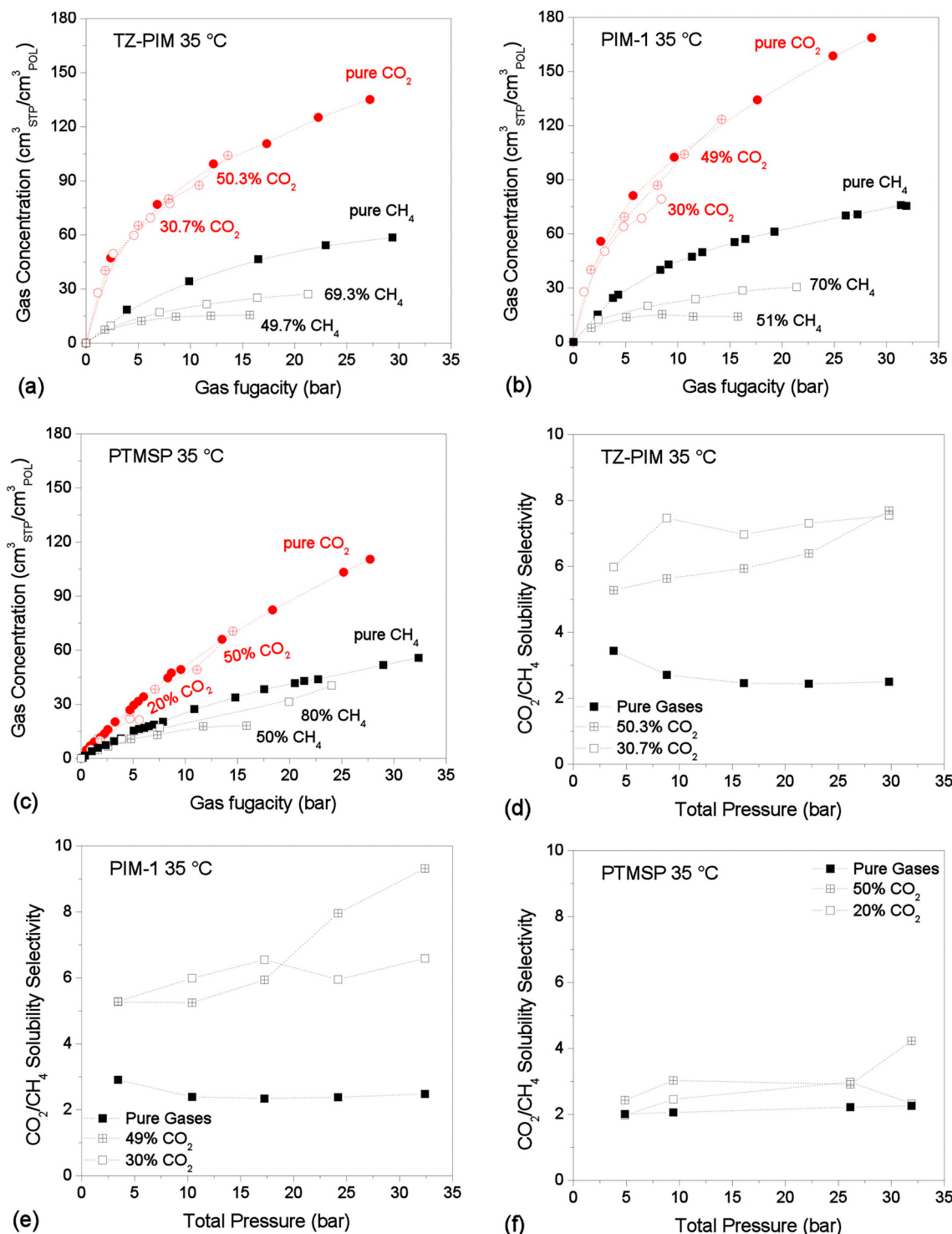


Fig. 3. – Comparison between the sorption isotherms of CO₂ and CH₄ in pure- and mixed-gas conditions at 35 °C in (a) TZ-PIM, (b) PIM-1 (data from Ref. [32]), (c) PTMSP (data from Ref. [31]). Solubility-selectivity in the ideal case (calculated with pure-gas concentration) and in the multicomponent case, at 35 °C in (d) TZ-PIM, (e) PIM-1 (data from Ref. [32]), (f) PTMSP (data from Ref. [31]).

In the case of PTMSP, the model is able to capture the fact that, in this material, the competitive effect is less pronounced than in the polymers of intrinsic microporosity. Average deviations between the model and the experimental data at 10%, 20% and 50% CO₂ are, respectively, 9%, 4%, 8% in the case of CO₂ and 2%, 8%, 13% in the case of CH₄. These values are very close to the average experimental confidence intervals for CO₂ (6%, 7% and 7% respectively), and generally lower than those of CH₄ (11%, 12%, 14% respectively).

The calculations were performed also at 25 °C and 50 °C for TZ-PIM and PIM-1 and the results can be seen in Fig. S1 and Fig. S2 of the Supporting Information file.

In the case of TZ-PIM at 25 °C, the CH₄ concentration is underestimated by the model at equimolar composition, where the average difference between the model and the experimental results is 30%. At 30.8 mol.% CO₂ and 11.5 mol.% CO₂ the average deviations between experimental and calculated CH₄ concentration are 14% and 3%

Table 1

Sanchez-Lacombe EoS pure component parameters used for NELF calculations.

	T^* (K)	p^* (MPa)	ρ^* (g/cm ³)	Ref.
PTMSP	610	380	1.125	[92]
PIM-1	872	523	1.438	[51]
TZ-PIM	550	800	1.657	[91]
CO ₂	300	630	1.515	[48]
CH ₄	215	250	0.500	[81]

respectively, while for CO₂ the deviations are 8%, 8% and 9% going from the CO₂-richer to the CO₂-poorer mixture. Average deviations at 50 °C are higher for CO₂ and lower for CH₄ compared to the 35 °C case: for CH₄ they are 5%, 6% and 4% increasing the CO₂ content from 10.6 to 50 mol.%, whereas for CO₂ they are 15%, 7% and 14.5%. These values are of the same order of the experimental confidence intervals (13%, 13%, 12%).

In the case of PIM-1 at 25 and 50 °C there is high agreement between the data and the model predictions for CO₂ at both temperatures and at all concentrations, with average deviations below 5%, while for CH₄ the agreement increases at higher temperatures. For instance, at 25 °C the highest relative deviation between model and experiments is 30% in the case of the equimolar mixture, while it is reduced to 4% at 50 °C respectively.

Another SL parameter set was reported in the literature for PTMSP ($T^* = 416$ K, $p^* = 405$ MPa, $\rho^* = 1.250$ g/cm³) [96], which was tested with respect to mixed-gas sorption calculations. With this alternative parameter set, it was possible to represent the pure gas sorption isotherms of CO₂ and CH₄ in PTMSP with indistinguishable results. The binary parameters used in this case are: $k_{CO_2,PTMSP} = 0.042$, $k_{CH_4,PTMSP} = -0.032$, $k_{sw,CO_2} = 0.015$ MPa⁻¹, $k_{sw,CH_4} = 0$ MPa⁻¹. The results of mixed-gas calculations performed with these parameters are not shown, for brevity, but were identical to those obtained with the parameters reported in [Tables 1 and 2](#).

NELF model predictions are sensitive to the dry polymer density value that is being considered [97], which affects significantly the values of the adjustable parameters employed to fit the experimental pure-gas sorption data. Taking into account the error bar in the density measurement, the ranges of variation of the adjustable parameters for the representation of pure CO₂ and CH₄ sorption in PIM-1 and TZ-PIM were determined, and they are reported in [Table S2](#) and [Table S3](#). Moving along the whole the density error bar, it was always possible to obtain an accurate representation of the pure-gas sorption data, by tuning the adjustable coefficients accordingly. It was found that a small deviation (~1%) of the dry polymer density value had a proportionally higher effect on the value of the binary parameter k_{ij} , which showed variations up to 100% in the case of CO₂ in PIM-1. On the other hand, the swelling coefficient k_{sw} was significantly less affected, with deviations ranging from 2% at 25 °C to 5% at 50 °C in the case of CO₂ in PIM-1.

The sensitivity of the mixed-gas predictions, associated with the error in the density measurement and the corresponding variability of

adjustable parameters, was subsequently assessed. The results are reported in the Supplementary Information file, in [Fig. S4](#) for the case of PIM-1 and in [Fig. S5](#) for the case of TZ-PIM, at 25, 35, 50 °C. The mixed-gas predictions are affected also by the adjustable parameters pertaining to the second gas. Remarkably, the results show a limited variability (below 2%), both for CO₂ and CH₄, at all compositions. Therefore, the mixed-gas calculations with the NELF model are robust with respect to a small perturbation of the initial density value, which is compensated by a variation of the adjustable coefficients, yielding consistent multicomponent results, when the same pure-gas representation is obtained with a different parameter set.

5.3. Solubility-selectivity

In this section the solubility-selectivity α^S is evaluated, making use of Eq. (12) with the mixed-gas concentrations calculated by the model. The obtained trends are compared with the experimental data in [Fig. 5](#). Only results at 35 °C are shown, for brevity. For the cases not shown, the general trends listed below were always followed, however quantitative agreement with the experimental data mirrors the results obtained for the sorption isotherms; the largest deviation is found at 25 °C for PIM-1 and amounts to 60% of the experimental value.

In all cases the solubility-selectivity is hardly dependent on the total pressure, in agreement with the experimental trends. In TZ-PIM and PIM-1, where the competitive effect is more pronounced, the solubility-selectivity increases as the molar fraction of CO₂ in the mixture increases: the maximum increase between the 10 and the 50 mol.% CO₂ cases is registered at high pressure and is 20% for TZ-PIM and 25% for PIM-1.

PTMSP exhibits a lower concentration dependence of the solubility-selectivity, with a maximum 12% increase when increasing CO₂ content of the mixture.

The same concentration dependence is displayed in all cases inspected: the solubility-selectivity is higher in the CO₂-richer mixtures, owing to the stronger competition. However, the two PIMs show a somewhat different, though weak, trend with respect to temperature (See [Fig. S5](#) in the supporting information file). PIM-1 predicted solubility-selectivity slightly decreases with increasing temperature, while that of TZ-PIM slightly increases, due to the different sorption enthalpies of the two gases in the materials.

5.4. Effects on mixed-gas permeability

A reliable modelling tool for mixed-gas solubility can prove useful also in decoupling the solubility and diffusivity effects that concur to determine the mixed-gas permselectivity. Indeed, mixed-gas permeation experiments often show a different behaviour from what is inferred from pure-gas data (ideal selectivity), and a more detailed understanding of the relative weight of the different phenomena in shaping the performance of a material can provide valuable insight and guide design considerations.

It must be pointed out that the following analysis is performed using permeability and sorption data measured for samples obtained through

Table 2

Binary interaction and swelling coefficients used in NELF calculations (temperature T is in K), obtained from the analysis of pure-gas sorption data from Refs. [31,33].

	k_{ij}	k_{sw} (MPa ⁻¹)
PTMSP	CO ₂	0.0876
	CH ₄	0.0580
PIM-1	CO ₂	$1.200 \cdot 10^{-4} T - 5.578 \cdot 10^{-2}$
	CH ₄	$8.000 \cdot 10^{-4} T - 2.685 \cdot 10^{-1}$
TZ-PIM	CO ₂	$-6.789 \cdot 10^{-4} T + 2.353 \cdot 10^{-1}$
	CH ₄	$8.000 \cdot 10^{-4} T - 3.085 \cdot 10^{-1}$
		0.0212
		0
		$-1.479 \cdot 10^{-3} T + 4.949 \cdot 10^{-1}$
		$-3.284 \cdot 10^{-4} T + 1.062 \cdot 10^{-1}$
		$-1.396 \cdot 10^{-3} T + 4.532 \cdot 10^{-1}$
		0.0131 (25 °C)
		0 (35–50 °C)

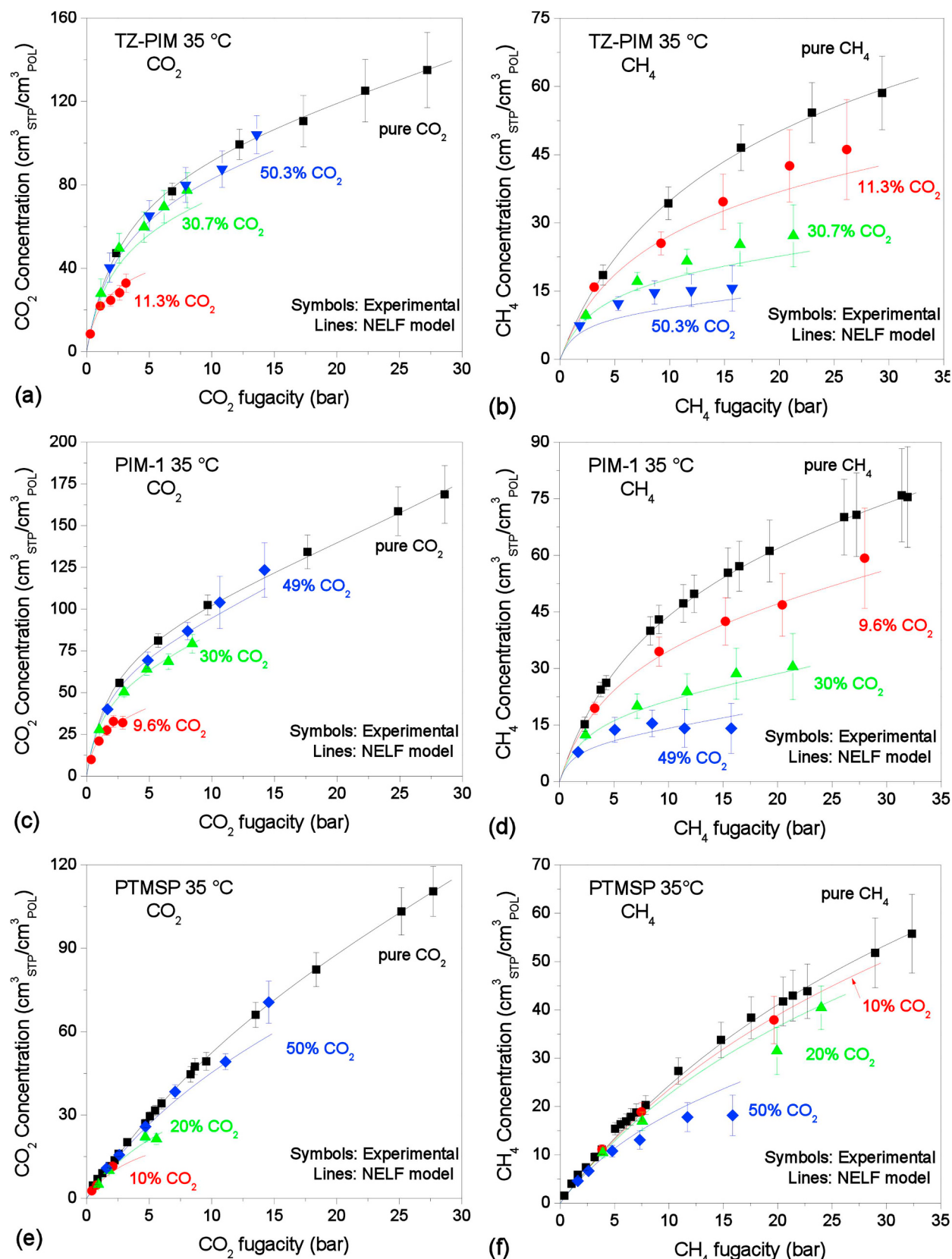


Fig. 4. Sorption isotherms of CO₂ and CH₄ at 35 °C TZ-PIM (a,b), PIM-1 (c,d), PTMSP (e,f), in pure- and mixed-gas conditions (Black squares: pure gas – Red circles: ~10% CO₂ mixture – Green triangles: ~30% CO₂ mixture – Blue diamonds: ~50% CO₂ mixture). Solid lines are NELF model predictions. (For interpretation of the references to colour in this figure legend, the reader is referred to the Web version of this article.)

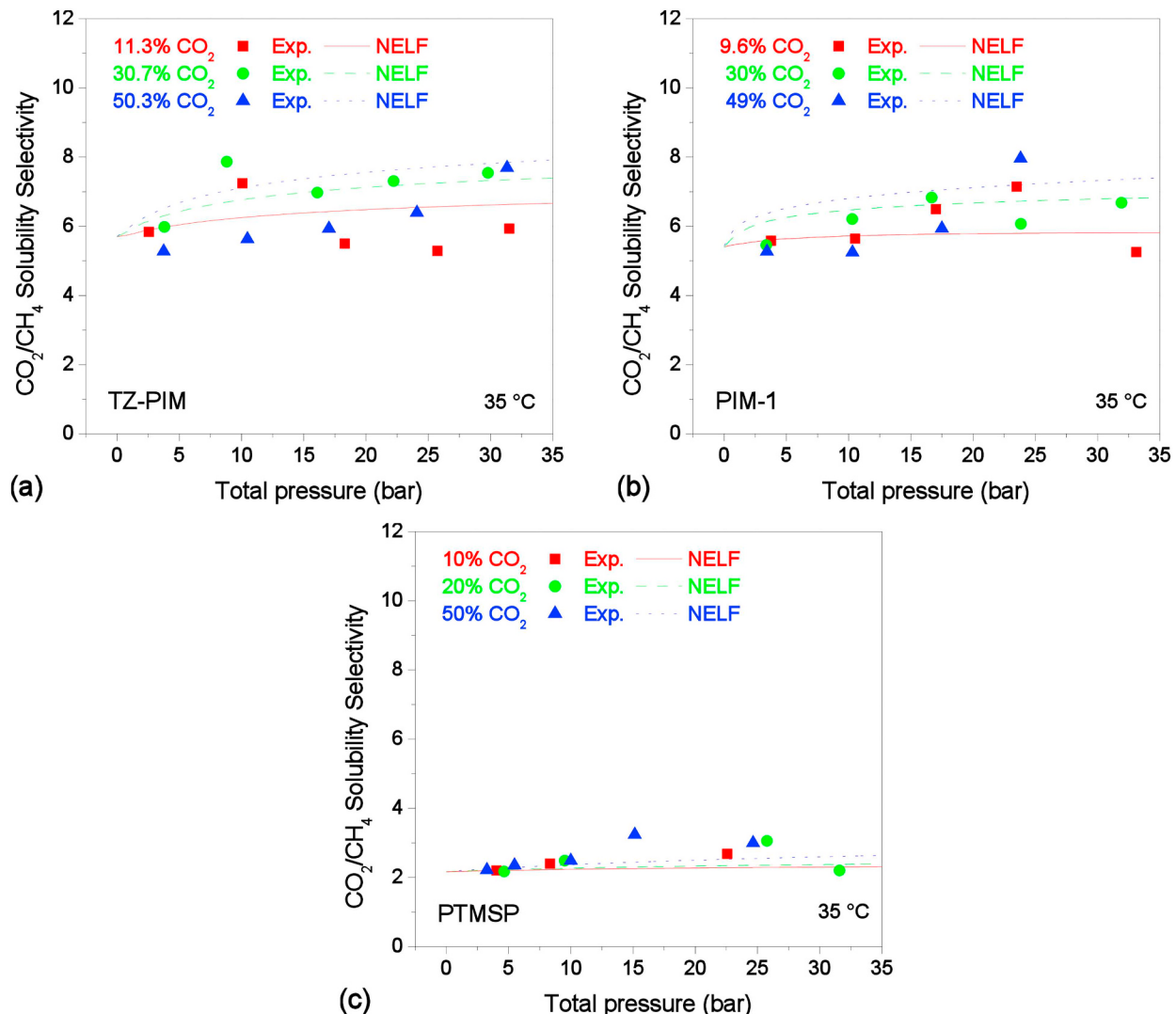


Fig. 5. – Solubility-selectivity of CO_2/CH_4 mixtures in (a) TZ-PIM, (b) PIM-1 (exp. data from Ref. [32]) and (c) PTMSP (exp. data from Ref. [31]) at 35°C . Symbols represent experimental data, lines are NELF calculations.

different protocols, for example in terms of casting solvent, thermal post-treatment, or ageing period, and this is known to be a source of variability in the transport properties of the membranes [79,98–100].

For PTMSP, no CO_2/CH_4 mixed-gas permeation results have been found in the literature. Its ideal selectivity for this gas couple is 2.10–2.15 [101,102] at 30°C and atmospheric pressure and diffusion coefficients, determined with the time-lag method at 30°C are $2.27 \cdot 10^{-5} \text{ cm}^2/\text{s}$ for CH_4 , and $2.21 \cdot 10^{-5} \text{ cm}^2/\text{s}$ for CO_2 [102]. Therefore, the ideal diffusivity-selectivity is close to one. The ideal solubility-selectivity at 35°C is equal to 2.2 and is almost pressure independent, while real solubility-selectivity increases slightly, from 2.2 up to 2.4 (10% CO_2 mixture) - 2.7 (50% CO_2 mixture) at high pressure. Competitive effects for this gas couple indeed have a weaker impact on the solubility of the two gases, compared, for example, to what was observed by Raharjo et al. for $\text{CH}_4/\text{nC}_4\text{H}_{10}$ in PTMSP [103].

Swaidan et al. [17] reported mixed-gas permeation experiments for a 50:50 CO_2/CH_4 mixture in PIM-1 at 35°C , up to 10 bar of CO_2 . The CO_2 permeability showed a decrease with increasing pressure, which is parallel to the observed decrease in the solubility coefficient with increasing pressure, both in pure- and mixed-gas conditions. Using Eq. (1) and the calculated solubility coefficients, CO_2 diffusivity can be estimated; it is thus possible to predict an average 4% decrease of CO_2 diffusivity, going from pure-gas to a 50:50 mixture at 35°C , which is

only a modest effect. CH_4 , on the other hand, shows as much as a 60% increase in permeability in mixed-gas conditions. The pure-gas permeability is almost pressure independent, while the mixed-gas one sharply increases with increasing pressure, which is a trend usually associated with the so-called plasticization effect. Since its solubility coefficient in mixed-gas conditions is significantly lower than the pure-gas one, this leads to the conclusion that its diffusivity is increased by a factor 2 to 5 over the pressure range inspected. The same effect was observed in MD simulations of mixed-gas CO_2/N_2 in a Thermally-Rearranged polymer [70] at 35°C : the simulated diffusion coefficient of N_2 exhibited a threefold increase in the presence of CO_2 , while that of CO_2 barely changed.

This is a synergistic effect, likely associated with CO_2 -induced swelling of the matrix, and overshadows the enhanced solubility-selectivity, leading to an overall 38% decrease in mixed-gas permselectivity, with respect to the ideal value [17]. In fact, in mixed-gas permeation conditions, the amount of CO_2 sorbed by the membrane is expected to be close to that of the pure-gas case, due to the little influence of competitive sorption effect for this gas, as highlighted by mixed-gas sorption experiments. Therefore, the polymer matrix will be diluted to a very similar extent and the CO_2 diffusivity is not expected to be significantly altered between the pure-gas and the mixed-gas cases. On the contrary, CH_4 is not capable of inducing the same dilation as

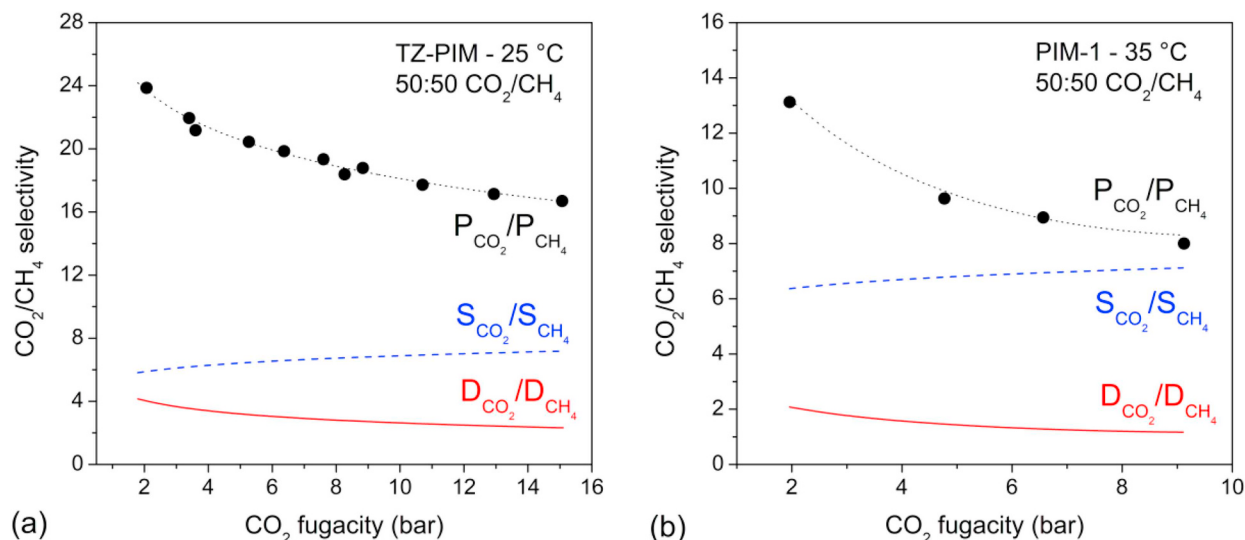


Fig. 6. – Permselectivity of 50:50 CO₂/CH₄ mixtures in (a) PIM-1 [17] and (b) TZ-PIM [75]. Black lines are interpolations of experimental data to guide the eye, dashed blue lines represent solubility-selectivity values calculated with NELF and solid red lines are diffusivity-selectivity values obtained with Eq. (2). (For interpretation of the references to colour in this figure legend, the reader is referred to the Web version of this article.)

CO₂. However, in the mixed-gas case, due to the swelling induced by the presence of a high concentration of CO₂ inside the membrane, CH₄ will be exposed to a significantly more dilated polymer matrix, and, therefore, it will diffuse faster with respect to the pure-gas case.

For TZ-PIM, Du et al. [75] have reported mixed-gas permselectivity data together for 50:50 and 80:20 CO₂/CH₄ mixtures at 25 °C up to 15 bar of CO₂. The accuracy of the models for mixed-gas selectivity in these conditions (25 °C) was lower, with respect to the previous analysis of PIM-1 at 35 °C, therefore the estimated diffusivity selectivity trend is expected to be affected correspondingly. However, the qualitative conclusions that can be drawn do not change. The decomposition of the permselectivity in its solubility and diffusivity components is reported in Fig. 6. The overall permselectivity in mixed-gas conditions is fairly similar to the ideal one (~22 at 25 °C and 4.4 bar [75]). It appears that TZ-PIM, characterized by a lower fractional free volume (FFV) value with respect to PIM-1 and a more rigid structure, with hydrogen bonding [75], better resists CO₂-induced swelling and also maintains some sieving capability in mixed-gas conditions, in addition to a solubility-selectivity enhancement due to competition.

As a result, for this material, pure- and mixed-gas CO₂/CH₄ permselectivity are very similar. The combination and relative weight of those effects can sometimes even lead to a higher permselectivity in mixed-gas conditions: the permselectivity for the CO₂/N₂ pair in this material, in the pressure range 0–17 bar, increased from ~30 to 25 in pure-gas conditions up to ~40–35 for a 50:50 CO₂/N₂ mixture [75] at 25 °C. This behaviour is even more pronounced in methyl tetrazole PIM (MTZ-PIM), a derivative of TZ-PIM, for which a twofold increase in permselectivity is witnessed in mixed-gas conditions for the CO₂/N₂ couple [104].

The CO₂-induced volume dilation can be estimated from Eq. (3) as a function of penetrant partial pressure, assuming isotropic swelling:

$$\frac{V - V_0}{V_0} = k_{sw} P \quad (13)$$

Using the swelling coefficients reported in Table 2, it is possible to calculate a volume change of 8% for PIM-1 at 35 °C and 20 bar (CO₂ uptake: 135 cm_{STP}³/cm_{pol}³), whereas for TZ-PIM in the same conditions the volume change is only 5%. The same CO₂ uptake (135 cm_{STP}³/cm_{pol}³) is attained for TZ-PIM at 31 bar, and corresponds to a volume change of 7%, consistent with the postulated higher resistance of TZ-PIM to CO₂ induced swelling.

Recently, CO₂/CH₄ diffusivity-selectivity in multicomponent conditions was determined experimentally for other materials [105,106]. Garrido et al. [106], using a combination of ¹³C NMR spectroscopy and pulsed-field gradient NMR, determined that, for an equimolar CO₂/CH₄ mixture in 6FDA-TMPDA polyimide, at 30 °C and a partial pressure of CO₂ of ~2.2 bar, the diffusivity-selectivity decreased from an ideal value of about 4 to approximately 2 in mixed-gas conditions. Similarly, Fraga et al. [105] measured in PIM-EA-TB a CO₂/CH₄ multicomponent diffusivity-selectivity value of ~2 on a wide range of compositions (10–50 mol.% CO₂), which is lower than the value of approximately 4 determined by Carta et al. [21] from pure-gas experiments. These values are in good agreement with those obtained through the solution-diffusion model analysis carried out here.

The interpretation of the upper-bound trade-off provided by Freeman et al. [107] attributes to the diffusivity-selectivity a predominant role. It is considered that, as the permeability of the faster gas decreases, the gain in permselectivity is associated with an increase in diffusivity-selectivity, due to enhanced sieving effects, while solubility-selectivity remains nearly invariant with permeability and free volume. Subsequent analysis recognized a correlation of the solubility-selectivity factor with free volume [108]; however, these analysis were performed using pure-gas data.

The joint analysis of mixed-gas sorption and permeation data performed here suggests that with ultrahigh free volume materials, like PIMs, the separation in actual multicomponent conditions is mainly driven by solubility, as the diffusivity-selectivity undergoes a drastic drop.

6. Conclusions

In this work the sorption of CO₂, CH₄ and of CO₂/CH₄ mixtures in TZ-PIM was measured at three different temperatures and three gas compositions. The results are in agreement with other mixed-gas sorption measurements present in the literature, and show that during mixed-gas sorption the solubility of both gases decreases with respect to the pure-gas case, due to competitive effects. However, the presence of CO₂ has a profound impact on CH₄ solubility, while CH₄ presence barely affects CO₂ sorption, even in mixtures with very high CH₄ content. This phenomenon has a positive influence on the performance of the materials, since it appreciably enhances the solubility-selectivity.

As the experimental investigation has shown, the separation

properties of glassy polymeric membranes are strongly influenced by temperature, pressure and mixture composition. It is possible to account for such effects on solubility using reliable and computationally inexpensive modelling tools, which require only pure-gas sorption isotherms as input and can provide a more representative description of the separation performance of a material than the ideal one, calculated with pure-gas data. In particular, the NELF model was used to calculate mixed-gas CO_2/CH_4 sorption isotherms in TZ-PIM and, for comparison, also in PIM-1 and PTMSP. The results of the calculations compared well with the experimental data measured in this work for TZ-PIM and with the literature ones for PIM-1 and PTMSP, demonstrating the ability of the model to adequately predict mixture effects.

The reduction in solubility due to competition when a second gas is present in the mixture reflects in a change in the solubility-selectivity of the materials, with respect to the value computed using pure-gas data (ideal solubility-selectivity). Solubility-selectivity was also calculated here in multicomponent conditions and the results compared well with the experimental findings for the three materials considered.

A combined analysis of multicomponent permeation and sorption data revealed that performance and materials design considerations based on pure-gas permeability/selectivity can be misleading in case of mixtures containing a highly sorbing component, like CO_2 . In these conditions, penetrant-induced swelling has a detrimental effect on the diffusivity-selectivity of the material and the separation becomes controlled by solubility differences. Therefore, materials capable of amplifying the competition effects, in order to achieve a more favourable sorption for one of the components in the mixture are expected to maintain a higher mixed-gas permselectivity.

Acknowledgements

Authors gratefully thank Eugenio Tacchini for his collaboration in the modelling section of this work. Authors would also like to acknowledge Ondřej Vopička for setting up the mixed-gas sorption equipment used in this work.

Appendix A. Supplementary data

Supplementary data to this article can be found online at <https://doi.org/10.1016/j.memsci.2019.05.026>.

References

- [1] M. Galizia, W.S. Chi, Z.P. Smith, T.C. Merkel, R.W. Baker, B.D. Freeman, 50th anniversary perspective: polymers and mixed matrix membranes for gas and vapor separation: a review and prospective opportunities, *Macromolecules* 50 (2017) 7809–7843, <https://doi.org/10.1021/acs.macromol.7b01718>.
- [2] Y. Zhang, J. Sunarso, S. Liu, R. Wang, Current status and development of membranes for CO_2/CH_4 separation: a review, *Int. J. Greenh. Gas Control* 12 (2013) 84–107, <https://doi.org/10.1016/j.ijggc.2012.10.009>.
- [3] D.F. Sanders, Z.P. Smith, R. Guo, L.M. Robeson, J.E. McGrath, D.R. Paul, B.D. Freeman, Energy-efficient polymeric gas separation membranes for a sustainable future: A review, *Polymer*; United Kingdom 54 (2013) 4729–4761 <https://doi.org/10.1016/j.polymer.2013.05.075>.
- [4] C.A. Scholes, G.W. Stevens, S.E. Kentish, Membrane gas separation applications in natural gas processing, *Fuel* 96 (2012) 15–28, <https://doi.org/10.1016/j.fuel.2011.12.074>.
- [5] L.M. Robeson, Correlation of separation factor versus permeability for polymeric membranes, *J. Membr. Sci.* 62 (1991) 165–185, [https://doi.org/10.1016/0376-7388\(91\)80060-J](https://doi.org/10.1016/0376-7388(91)80060-J).
- [6] L.M. Robeson, The upper bound revisited, *J. Membr. Sci.* 320 (2008) 390–400, <https://doi.org/10.1016/j.memsci.2008.04.030>.
- [7] H.B. Park, J. Kamcev, L.M. Robeson, M. Elimelech, B.D. Freeman, Maximizing the right stuff: the trade-off between membrane permeability and selectivity, *Science* 355 (2017) 1138–1148, <https://doi.org/10.1126/science.aab0530>.
- [8] H. Lin, B.D. Freeman, Materials selection guidelines for membranes that remove CO_2 from gas mixtures, *J. Mol. Struct.* 739 (2005) 57–74, <https://doi.org/10.1016/j.molstruc.2004.07.045>.
- [9] S. Wang, X. Li, H. Wu, Z. Tian, Q. Xin, G. He, D. Peng, S. Chen, Y. Yin, Z. Jiang, M.D. Guiver, Advances in high permeability polymer-based membrane materials for CO_2 separations, *Energy Environ. Sci.* 9 (2016) 1863–1890, <https://doi.org/10.1039/c6ee00811a>.
- [10] S. Luo, Q. Zhang, L. Zhu, H. Lin, B.A. Kazanowska, C.M. Doherty, A.J. Hill, P. Gao, R. Guo, Highly selective and permeable microporous polymer membranes for hydrogen purification and CO_2 removal from natural gas, *Chem. Mater.* 30 (2018) 5322–5332, <https://doi.org/10.1021/acs.chemmater.8b02102>.
- [11] W.J. Koros, C. Zhang, Materials for next-generation molecularly selective synthetic membranes, *Nat. Mater.* 16 (2017) 289–297, <https://doi.org/10.1038/nmat4805>.
- [12] M. Carta, M. Croad, R. Malpass-Evans, J.C. Jansen, P. Bernardo, G. Clarizia, K. Friess, M. Lanč, N.B. McKeown, Triptycene induced enhancement of membrane gas selectivity for microporous Tröger's base polymers, *Adv. Mater.* 26 (2014) 3526–3531 <https://doi.org/10.1002/adma>.
- [13] Y. He, F.M. Benedetti, S. Lin, C. Liu, Y. Zhao, H.-Z. Ye, T. Van Voorhis, M.G. De Angelis, T.M. Swager, Z.P. Smith, Polymers with side chain porosity for ultra-permeable and plasticization resistant materials for gas separations, *Adv. Mater.* (2019) 1807871, <https://doi.org/10.1002/adma.201807871>.
- [14] P.M. Budd, B.S. Ghanem, S. Makhsheed, N.B. McKeown, K.J. Msayib, C.E. Tattershall, Polymers of intrinsic microporosity (PIMs): robust, solution-processable, organic nanoporous materials, *Chem. Commun.* (2004) 230–231, <https://doi.org/10.1039/b311764b>.
- [15] P.M. Budd, K.J. Msayib, C.E. Tattershall, B.S. Ghanem, K.J. Reynolds, N.B. McKeown, D. Fritsch, Gas separation membranes from polymers of intrinsic microporosity, *J. Membr. Sci.* 251 (2005) 263–269, <https://doi.org/10.1016/j.memsci.2005.01.009>.
- [16] N.B. McKeown, P.M. Budd, Exploitation of intrinsic microporosity in polymer-based materials, *Macromolecules* 43 (2010) 5163–5176, <https://doi.org/10.1021/ma1006396>.
- [17] R. Swaidan, B.S. Ghanem, E. Litwiller, I. Pinna, Pure- and mixed-gas CO_2/CH_4 separation properties of PIM-1 and an amidoxime-functionalized PIM-1, *J. Membr. Sci.* 457 (2014) 95–102, <https://doi.org/10.1016/j.memsci.2014.01.055>.
- [18] I. Rose, C.G. Bezzu, M. Carta, B. Comesáñ-Gándara, E. Lasseguette, M.C. Ferrari, P. Bernardo, G. Clarizia, A. Fuoco, J.C. Jansen, K.E. Hart, T.P. Liyan-Arachchi, C.M. Colina, N.B. McKeown, Polymer ultrapermeability from the inefficient packing of 2D chains, *Nat. Mater.* 16 (2017) 1–39, <https://doi.org/10.1038/nmat4939>.
- [19] B.S. Ghanem, R. Swaidan, E. Litwiller, I. Pinna, Ultra-microporous triptycene-based polyimide membranes for high-performance gas separation, *Adv. Mater.* 26 (2014) 3688–3692, <https://doi.org/10.1002/adma.201306229>.
- [20] B.S. Ghanem, R. Swaidan, X. Ma, E. Litwiller, I. Pinna, Energy-efficient hydrogen separation by AB-type ladder-polymer molecular sieves, *Adv. Mater.* 26 (2014) 6696–6700, <https://doi.org/10.1002/adma.201401328>.
- [21] M. Carta, R. Malpass-Evans, M. Croad, Y. Rogan, J.C. Jansen, P. Bernardo, F. Bazzarelli, N.B. McKeown, An efficient polymer molecular sieve for membrane gas separations, *Science* 339 (2013) 303–307, <https://doi.org/10.1126/science.1228032>.
- [22] S. Kim, Y.M. Lee, Rigid and microporous polymers for gas separation membranes, *Prog. Polym. Sci.* 43 (2015) 1–32, <https://doi.org/10.1016/j.progpolymsci.2014.10.005>.
- [23] S.H. Han, H.J. Kwon, K.Y. Kim, J.G. Seong, C.H. Park, S. Kim, C.M. Doherty, A.W. Thornton, A.J. Hill, A.E. Lozano, K. a Berchtold, Y.M. Lee, Tuning microcavities in thermally rearranged polymer membranes for CO_2 capture, *Phys. Chem. Chem. Phys.* 14 (2012) 4365–4373, <https://doi.org/10.1039/c2cp23729f>.
- [24] Y.-R. Chen, L.-H. Chen, K.-S. Chang, T.-H. Chen, Y.-F. Lin, K.-L. Tung, Structural characteristics and transport behavior of triptycene-based PIMs membranes: a combination study using ab initio calculation and molecular simulations, *J. Membr. Sci.* 514 (2016) 114–124, <https://doi.org/10.1016/j.memsci.2016.04.063>.
- [25] K.-S. Chang, K.-L. Tung, Y.-F. Lin, H.-Y. Lin, Molecular modelling of polyimides with intrinsic microporosity: from structural characteristics to transport behaviour, *RSC Adv.* 3 (2013) 10403–10413, <https://doi.org/10.1039/c3ra40196k>.
- [26] E. Tocci, L. De Lorenzo, P. Bernardo, G. Clarizia, F. Bazzarelli, N.B. McKeown, M. Carta, R. Malpass-Evans, K. Friess, K. Pilnáček, M. Lanč, Y.P. Yampolskii, L. Stránníková, V. Štancarovič, M. Mauri, J.C. Jansen, Molecular modeling and gas permeation properties of a polymer of intrinsic microporosity composed of ethanoanthracene and Tröger's base units, *Macromolecules* 47 (2014) 7900–7916, <https://doi.org/10.1021/ma501469m>.
- [27] G.S. Larsen, P. Lin, K.E. Hart, C.M. Colina, Molecular simulations of PIM-1-like polymers of intrinsic microporosity, *Macromolecules* 44 (2011) 6944–6951, <https://doi.org/10.1021/ma200345v>.
- [28] T.M. Madkour, J.E. Mark, Molecular modeling investigation of the fundamental structural parameters of polymers of intrinsic microporosity for the design of tailor-made ultra-permeable and highly selective gas separation membranes, *J. Membr. Sci.* 431 (2013) 37–46, <https://doi.org/10.1016/j.memsci.2012.12.033>.
- [29] J.K. Moore, M.D. Guiver, N. Du, S.E. Hayes, M.S. Conradi, Molecular motions of adsorbed CO_2 on a tetrazole-functionalized pim polymer studied with ^{13}C NMR, *J. Phys. Chem. C* 117 (2013) 22995–22999, <https://doi.org/10.1021/jp4084234>.
- [30] R.W. Baker, B.T. Low, Gas separation membrane materials: a perspective, *Macromolecules* 47 (2014) 6999–7013, <https://doi.org/10.1021/ma501488s>.
- [31] O. Vopička, M.G. De Angelis, G.C. Sarti, Mixed gas sorption in glassy polymeric membranes: I. CO_2/CH_4 and n-C₄/CH₄ mixtures sorption in poly(1-trimethylsilyl-1-propyne) (PTMSP), *J. Membr. Sci.* 449 (2013) 97–108, <https://doi.org/10.1016/j.memsci.2013.06.065>.
- [32] O. Vopička, M.G. De Angelis, N. Du, N. Li, M.D. Guiver, G.C. Sarti, Mixed gas sorption in glassy polymeric membranes: II. CO_2/CH_4 mixtures in a polymer of intrinsic microporosity (PIM-1), *J. Membr. Sci.* 459 (2014) 264–276, <https://doi.org/10.1016/j.memsci.2014.02.003>.
- [33] A.E. Gameda, M.G. De Angelis, N. Du, N. Li, M.D. Guiver, G.C. Sarti, Mixed gas sorption in glassy polymeric membranes. III. CO_2/CH_4 mixtures in a polymer of

- intrinsic microporosity (PIM-1): effect of temperature, *J. Membr. Sci.* 524 (2017) 746–757, <https://doi.org/10.1016/j.memsci.2016.11.053>.
- [34] K.L. Gleason, Z.P. Smith, Q. Liu, D.R. Paul, B.D. Freeman, Pure- and mixed-gas permeation of CO₂ and CH₄ in thermally rearranged polymers based on 3,3'-di-hydroxy-4,4'-diamino-biphenyl (HAB) and 2,2'-bis-(3,4-dicarboxyphenyl) hexa-fluoropropane dianhydride (6FDA), *J. Membr. Sci.* 475 (2015) 204–214, <https://doi.org/10.1016/j.memsci.2014.10.014>.
- [35] J.G. Wijmans, R.W. Baker, The solution-diffusion model: a review, *J. Membr. Sci.* 107 (1995) 1–21.
- [36] P. Meares, The diffusion of gases through polyvinyl acetate1, *J. Am. Chem. Soc.* 482 (1954), <https://doi.org/10.1021/ja01642a015>.
- [37] P. Meares, The solubilities of gases in polyvinyl acetate, *Trans. Faraday Soc.* 54 (1957) 40–46.
- [38] R.M. Barrer, J.A. Barrie, J. Slater, Sorption and diffusion in ethyl cellulose. Part III. Comparison between ethyl cellulose and rubber, *J. Polym. Sci. XXVII* (1958) 177–197.
- [39] W.R. Vieth, P.M. Tam, A.S. Michaels, Dual sorption mechanisms in glassy polystyrene, *J. Colloid Interface Sci.* 22 (1966) 360–370, [https://doi.org/10.1016/0021-9797\(66\)90016-6](https://doi.org/10.1016/0021-9797(66)90016-6).
- [40] W.R. Vieth, J.M. Howell, J.H. Hsieh, Dual sorption theory, *J. Membr. Sci.* 1 (1976) 177–220, [https://doi.org/10.1016/S0376-7388\(00\)82267-X](https://doi.org/10.1016/S0376-7388(00)82267-X).
- [41] W.J. Koros, D.R. Paul, Carbon dioxide sorption and transport in polycarbonate, *J. Polym. Sci., Polym. Phys. Ed.* 14 (1976) 687–702, <https://doi.org/10.1002/pol.1976.180140410>.
- [42] D.R. Paul, W.J. Koros, Effect of partially immobilizing sorption on permeability and the diffusion time lag, *J. Polym. Sci. Polym. Phys. Ed* 14 (1976) 675–685, <https://doi.org/10.1002/pol.1976.180140409>.
- [43] G.H. Fredrickson, E. Helfand, Dual-mode transport of penetrants in glassy polymers, *Macromolecules* 18 (1985) 2201–2207, <https://doi.org/10.1021/ma00153a024>.
- [44] W.J. Koros, Model for sorption of mixed gases in glassy polymers, *J. Polym. Sci. Polym. Phys. Ed* 18 (1980) 981–992, <https://doi.org/10.1002/pol.1980.180180506>.
- [45] E. Ricci, M.G. De Angelis, Modelling mixed gas sorption in glassy polymers for CO₂ removal: a sensitivity analysis of the dual Mode sorption model, *Membranes* 9 (2019) 8.
- [46] R.H. Lacombe, I.C. Sanchez, Statistical thermodynamics of fluid mixtures, *J. Phys. Chem.* 80 (1976) 2568–2580, <https://doi.org/10.1021/j100564a009>.
- [47] W.G. Chapman, K.E. Gubbins, G. Jackson, M. Radosz, SAFT: equation-of-state solution model for associating fluids, *Fluid Phase Equilib.* 52 (1989) 31–38, [https://doi.org/10.1016/0378-3812\(89\)80308-5](https://doi.org/10.1016/0378-3812(89)80308-5).
- [48] F. Doghieri, G.C. Sarti, Nonequilibrium lattice fluids: a predictive model for the solubility in glassy polymers, *Macromolecules* 29 (1996) 7885–7896, <https://doi.org/10.1021/ma951366c>.
- [49] M. Minelli, F. Doghieri, Predictive model for gas and vapor solubility and swelling in glassy polymers I: application to different polymer/penetrant systems, *Fluid Phase Equilib.* 381 (2014) 1–11, <https://doi.org/10.1016/j.fluid.2014.08.010>.
- [50] F. Doghieri, M. Quinzi, D.G. Rethwisch, G.C. Sarti, Predicting gas solubility in glassy polymers through nonequilibrium EOS, *Adv. Mater. Membr. Sep. American Chemical Society, Washington, DC, USA, 2004*, pp. 74–90, , <https://doi.org/10.1021/bk-2004-0876.ch005>.
- [51] M. Minelli, K. Friess, O. Vopička, M.G. De Angelis, Modeling gas and vapor sorption in a polymer of intrinsic microporosity (PIM-1), *Fluid Phase Equilib.* 347 (2013) 35–44, <https://doi.org/10.1016/j.fluid.2013.03.003>.
- [52] M. Minelli, S. Campagnoli, M.G. De Angelis, F. Doghieri, G.C. Sarti, Predictive model for the solubility of fluid mixtures in glassy polymers, *Macromolecules* 44 (2011) 4852–4862, <https://doi.org/10.1021/ma200602d>.
- [53] M.P. Allen, D.J. Tildesley, *Computer Simulation of Liquids*, Clarendon Press, Wotton-under-Edge, UK, 1989.
- [54] A.Z. Panagiotopoulos, U.W. Suter, R.C. Reid, Phase diagrams of nonideal fluid mixtures from Monte Carlo simulation, *Ind. Eng. Chem. Fundam.* 25 (1986) 525–535, <https://doi.org/10.1021/i100024a012>.
- [55] B. Widom, Some topics in the theory of fluids, *J. Chem. Phys.* 39 (1963) 2808–2812, <https://doi.org/10.1121/1.418538>.
- [56] G.C. Boulougouris, I.G. Economou, D.N. Theodorou, On the calculation of the chemical potential using the particle deletion scheme, *Mol. Phys.* 96 (1999) 905–913, <https://doi.org/10.1080/00268979909483030>.
- [57] M.R. Siegert, M. Heuchel, D. Hofmann, A generalized direct-particle-deletion scheme for the calculation of chemical potential and solubilities of small- and medium-sized molecules in amorphous polymers, *J. Comput. Chem.* 28 (2007) 877–889, <https://doi.org/10.1002/jcc.20594>.
- [58] G. Kupgan, L.J. Abbott, K.E. Hart, C.M. Colina, Modeling amorphous microporous polymers for CO₂ capture and separations, *Chem. Rev.* 118 (2018) 5488–5538, <https://doi.org/10.1021/acs.chemrev.7b00691>.
- [59] K.E. Hart, C.M. Colina, Estimating gas permeability and permselectivity of microporous polymers, *J. Membr. Sci.* 468 (2014) 259–268, <https://doi.org/10.1016/j.memsci.2014.06.017>.
- [60] K.E. Hart, L.J. Abbott, N.B. McKeown, C.M. Colina, Toward effective CO₂/CH₄ separations by sulfur-containing PIMs via predictive molecular simulations, *Macromolecules* 46 (2013) 5371–5380, <https://doi.org/10.1021/ma400334b>.
- [61] M. Heuchel, D. Fritsch, P.M. Budd, N.B. McKeown, D. Hofmann, Atomistic packing model and free volume distribution of a polymer with intrinsic microporosity (PIM-1), *J. Membr. Sci.* 318 (2008) 84–99, <https://doi.org/10.1016/j.memsci.2008.02.038>.
- [62] A.A. Gusev, S. Arizzi, U.W. Suter, D.J. Moll, Dynamics of light gases in rigid matrices of dense polymers, *J. Chem. Phys.* 99 (1993) 2221–2227, <https://doi.org/10.1063/1.465283>.
- [63] A.A. Gusev, U.W. Suter, Dynamics of small molecules in dense polymers subject to thermal motion, *J. Chern. Phys.* 99 (1993) 2228–2234, <https://doi.org/10.1063/1.466198>.
- [64] W. Fang, L. Zhang, J. Jiang, Polymers of intrinsic microporosity for gas permeation: a molecular simulation study, *Mol. Simul.* 36 (2010) 992–1003, <https://doi.org/10.1080/08927022.2010.498828>.
- [65] W. Fang, L. Zhang, J. Jiang, Gas permeation and separation in functionalized polymers of intrinsic microporosity: a combination of molecular simulations and ab initio calculations, *J. Phys. Chem. C* 115 (2011) 14123–14130, <https://doi.org/10.1021/jp204193g>.
- [66] G. Kupgan, A.G. Demidov, C.M. Colina, Plasticization behavior in polymers of intrinsic microporosity (PIM-1): a simulation study from combined Monte Carlo and molecular dynamics, *J. Membr. Sci.* 565 (2018) 95–103, <https://doi.org/10.1016/j.memsci.2018.08.004>.
- [67] O. Hölick, M. Böhning, M. Heuchel, M.R. Siegert, D. Hofmann, Gas sorption isotherms in swelling glassy polymers - Detailed atomistic simulations, *J. Membr. Sci.* 428 (2013) 523–532, <https://doi.org/10.1016/j.memsci.2012.10.023>.
- [68] H. Frentrup, K.E. Hart, C.M. Colina, E.A. Müller, In silico determination of gas permeabilities by non-equilibrium molecular dynamics: CO₂ and He through PIM-1, *Membranes* 5 (2015) 99–119, <https://doi.org/10.3390/membranes5010099>.
- [69] D.N. Theodorou, *Principles of molecular simulation of gas transport in polymers, Materials Science of Membranes for Gas and Vapor Separation*, John Wiley & Sons, Hoboken, NJ, USA, 2006, pp. 49–94.
- [70] C. Rizzuto, A. Caravella, A. Brunetti, C.H. Park, Y.M. Lee, E. Drioli, G. Barbieri, E. Tocci, Sorption and Diffusion of CO₂/N₂ in gas mixture in thermally-rearranged polymeric membranes: a molecular investigation, *J. Membr. Sci.* 528 (2017) 135–146, <https://doi.org/10.1016/j.memsci.2017.01.025>.
- [71] A.L. Myers, J.M. Prausnitz, Thermodynamics of mixed-gas adsorption, *AIChE J.* 11 (1965) 121–127.
- [72] S. Neyertz, D. Brown, Air sorption and separation by polymer films at the molecular level, *Macromolecules* 51 (2018) 7077–7092, <https://doi.org/10.1021/acs.macromol.8b01423>.
- [73] I. Tanis, D. Brown, S. Neyertz, R. Heck, R. Mercier, M. Vaidya, J.P. Ballague, A comparison of pure and mixed-gas permeation of nitrogen and methane in 6FDA-based polyimides as studied by molecular dynamics simulations, *Comput. Mater. Sci.* 141 (2018) 243–253, <https://doi.org/10.1016/j.commatsci.2017.09.028>.
- [74] G.C. Sarti, F. Doghieri, Predictions of the solubility of gases in glassy polymers based on the NELF model, *Chem. Eng. Sci.* 53 (1998) 3435–3447, [https://doi.org/10.1016/S0009-2590\(98\)00143-2](https://doi.org/10.1016/S0009-2590(98)00143-2).
- [75] N. Du, H.B. Park, G.P. Robertson, M.M. Dal-Cin, T. Visser, L. Scoles, M.D. Guiver, Polymer nanosieve membranes for CO₂-capture applications, *Nat. Mater.* 10 (2011) 372–375, <https://doi.org/10.1038/nmat2989>.
- [76] *ASTM Standard Test Methods for Density and Specific Gravity (Relative Density) of Plastics by Displacement*, ASTM International, West Conshohocken, 1993(n.d.).
- [77] E.S. Sanders, W.J. Koros, H.B. Hopfenberg, V.T. Stannett, Mixed gas sorption in glassy polymers: equipment design considerations and preliminary results, *J. Membr. Sci.* 13 (1983) 161–174, [https://doi.org/10.1016/S0376-7388\(00\)80159-3](https://doi.org/10.1016/S0376-7388(00)80159-3).
- [78] S.S. Jordan, W.J. Koros, A free volume distribution model of gas sorption and dilation in glassy polymers, *Macromolecules* 28 (1995) 2228–2235, <https://doi.org/10.1021/ma00111a017>.
- [79] D.S. Pope, G.K. Fleming, W.J. Koros, Effect of various exposure histories on sorption and dilation in a family of polycarbonates, *Macromolecules* 23 (1990) 2988–2994, <https://doi.org/10.1021/ma00213a029>.
- [80] M.G. De Angelis, T.C. Merkel, V.I. Bondar, B.D. Freeman, F. Doghieri, G.C. Sarti, Hydrocarbon and fluorocarbon solubility and dilation in poly(dimethylsiloxane): comparison of experimental data with predictions of the Sanchez-Lacombe equation of state, *J. Polym. Sci., Part B: Polym. Phys.* 37 (1999) 3011–3026, <https://doi.org/10.1021/ma0106090>.
- [81] F. Doghieri, G.C. Sarti, Predicting the low pressure solubility of gases and vapors in glassy polymers by the NELF model, *J. Membr. Sci.* 147 (1998) 73–86, [https://doi.org/10.1016/S0376-7388\(98\)00123-9](https://doi.org/10.1016/S0376-7388(98)00123-9).
- [82] I.C. Sanchez, R.H. Lacombe, An elementary molecular theory of classical fluids. Pure fluids, *J. Phys. Chem.* 80 (1976) 2352–2362, <https://doi.org/10.1021/j100562a008>.
- [83] I.C. Sanchez, R.H. Lacombe, Statistical thermodynamics of polymer solutions, *Macromolecules* 11 (1978) 1145–1156 <http://pubs.acs.org/doi/pdf/10.1021/ma60066a017>, Accessed date: 26 June 2017.
- [84] D. Peng, D.B. Robinson, A new two-constant equation of state, *Ind. Eng. Chem. Fundam.* 15 (1976) 59–64, <https://doi.org/10.1021/i160057a011>.
- [85] S.I. Sandler, *Chemical, Biochemical, and Engineering Thermodynamics*, fifth ed., John Wiley & Sons, Hoboken, NJ, USA, 2017.
- [86] P.M. Budd, N.B. McKeown, B.S. Ghanem, K.J. Msayib, D. Fritsch, L. Starannikova, N. Belov, O. Sanfirova, Y. Yampolskii, V. Shantarovich, Gas permeation parameters and other physicochemical properties of a polymer of intrinsic microporosity: polybenzodioxane PIM-1, *J. Membr. Sci.* 325 (2008) 851–860, <https://doi.org/10.1016/j.memsci.2008.09.010>.
- [87] R.R. Tiwari, J. Jin, B.D. Freeman, D.R. Paul, Physical aging, CO₂ sorption and plasticization in thin films of polymer with intrinsic microporosity (PIM-1), *J. Membr. Sci.* 537 (2017) 362–371, <https://doi.org/10.1016/j.memsci.2017.04.069>.
- [88] N. Du, G.P. Robertson, J. Song, I. Pinna, M.D. Guiver, High-performance carboxylated polymers of intrinsic microporosity (PIMs) with tunable gas transport properties, *Macromolecules* 42 (2009) 6038–6043, <https://doi.org/10.1021/ma9009017>.

- [89] H. Yin, Y.Z. Chua, B. Yang, C. Schick, W.J. Harrison, P.M. Budd, M. Böhning, A. Schönhalz, First clear-cut experimental evidence of a glass transition in a polymer with intrinsic microporosity: PIM-1, *J. Phys. Chem. Lett.* 9 (2018) 2003–2008, <https://doi.org/10.1021/acs.jpclett.8b00422>.
- [90] M.G. De Angelis, G.C. Sarti, Solubility of gases and liquids in glassy polymers, *Annu. Rev. Chem. Biomol. Eng.* 2 (2011) 97–120, <https://doi.org/10.1146/annurev-chembioeng-061010-114247>.
- [91] M. Minelli, G.C. Sarti, Elementary prediction of gas permeability in glassy polymers, *J. Membr. Sci.* 521 (2017) 73–83, <https://doi.org/10.1016/j.memsci.2016.09.001>.
- [92] M.G. Baschetti, M. Ghisellini, M. Quinzii, F. Doghieri, P. Stagnaro, G. Costa, G.C. Sarti, Effects on sorption and diffusion in PTMSP and TMSP/TMSE copolymers of free volume changes due to polymer ageing, *J. Mol. Struct.* 739 (2005) 75–86, <https://doi.org/10.1016/j.molstruc.2004.08.027>.
- [93] R.L. de Miranda, J. Kruse, K. Rätzke, F. Faupel, D. Fritsch, V. Abetz, P.M. Budd, J.D. Selbie, N.B. McKeown, B.S. Ghanem, Unusual temperature dependence of the positron lifetime in a polymer of intrinsic microporosity, *Phys. Status Solidi Rapid Res. Lett.* 1 (2007) 190–192, <https://doi.org/10.1002/pssr.200701116>.
- [94] K. Golzar, H. Modarress, S. Amjad-Iranagh, Separation of gases by using pristine, composite and nanocomposite polymeric membranes: a molecular dynamics simulation study, *J. Membr. Sci.* 539 (2017) 238–256, <https://doi.org/10.1016/j.memsci.2017.06.010>.
- [95] L.J. Abbott, K.E. Hart, C.M. Colina, Polymatic: a generalized simulated polymerization algorithm for amorphous polymers, *Theor. Chem. Acc.* 132 (2013) 1–19, <https://doi.org/10.1007/s00214-013-1334-z>.
- [96] M.G. De Angelis, G.C. Sarti, Solubility and diffusivity of gases in mixed matrix membranes containing hydrophobic fumed silica: correlations and predictions based on the NELF model, *Ind. Eng. Chem. Res.* 47 (2008) 5214–5226, <https://doi.org/10.1021/ie0714910>.
- [97] M. Galizia, M.G. De Angelis, G.C. Sarti, Sorption of hydrocarbons and alcohols in addition-type poly(trimethyl silyl norbornene) and other high free volume glassy polymers. II: NELF model predictions, *J. Membr. Sci.* 405 (2012) 201–211, <https://doi.org/10.1016/j.memsci.2012.03.009>.
- [98] R. Guan, H. Dai, C. Li, J. Liu, J. Xu, Effect of casting solvent on the morphology and performance of sulfonated polyethersulfone membranes, *J. Membr. Sci.* 277 (2006) 148–156, <https://doi.org/10.1016/j.memsci.2005.10.025>.
- [99] L. Shao, T.S. Chung, G. Wensley, S.H. Goh, K.P. Pramoda, Casting solvent effects on morphologies, gas transport properties of a novel 6FDA/PMDA-TMMDA copolyimide membrane and its derived carbon membranes, *J. Membr. Sci.* 244 (2004) 77–87, <https://doi.org/10.1016/j.memsci.2004.07.005>.
- [100] C.H. Park, E. Tocci, Y.M. Lee, E. Drioli, Thermal treatment effect on the structure and property change between hydroxy-containing polyimides (HPIs) and thermally rearranged polybenzoxazole (TR-PBO), *J. Phys. Chem. B* 116 (2012) 12864–12877, <https://doi.org/10.1021/jp307365y>.
- [101] K. Nagai, T. Masuda, T. Nakagawa, B.D. Freeman, I. Pinna, Poly[1-(trimethylsilyl)-1-propyne] and related polymers: synthesis, properties and functions, *Prog. Polym. Sci.* 26 (2001) 721–798, [https://doi.org/10.1016/S0079-6700\(01\)00008-9](https://doi.org/10.1016/S0079-6700(01)00008-9).
- [102] Y. Ichiraku, S.A. Stern, T. Nakagawa, An investigation of the high gas permeability of poly(1-trimethylsilyl-1-propyne), *J. Membr. Sci.* 34 (1987) 5–18, [https://doi.org/10.1016/S0376-7388\(00\)80017-4](https://doi.org/10.1016/S0376-7388(00)80017-4).
- [103] R.D. Raharjo, B.D. Freeman, E.S. Sanders, Pure and mixed gas CH₄ and n-C₄H₁₀ sorption and dilation in poly(1-trimethylsilyl-1-propyne), *Polymer (Guildf)* 48 (2007) 6097–6114, <https://doi.org/10.1016/j.polym.2007.07.057>.
- [104] N. Du, G.P. Robertson, M.M. Dal-Cin, L. Scoles, M.D. Guiver, Polymers of intrinsic microporosity (PIMs) substituted with methyl tetrazole, *Polymer (Guildf)* 53 (2012) 4367–4372, <https://doi.org/10.1016/j.polym.2012.07.055>.
- [105] S.C. Fraga, M. Monteleone, M. Lanč, E. Esposito, A. Fuoco, L. Giorno, K. Pilnáček, K. Friess, M. Carta, N.B. McKeown, P. Izák, Z. Petrusová, J.G. Crespo, C. Brazinha, J.C. Jansen, A novel time lag method for the analysis of mixed gas diffusion in polymeric membranes by on-line mass spectrometry: method development and validation, *J. Membr. Sci.* 561 (2018) 39–58, <https://doi.org/10.1016/j.memsci.2018.04.029>.
- [106] L. Garrido, C. García, M. López-González, B. Comesáñ-Gándara, Á.E. Lozano, J. Guzmán, Determination of gas transport coefficients of mixed gases in 6FDA-TMPDA polyimide by NMR spectroscopy, *Macromolecules* 50 (2017) 3590–3597, <https://doi.org/10.1021/acs.macromol.7b00384>.
- [107] B.D. Freeman, Basis of permeability/selectivity tradeoff relations in polymeric gas separation membranes, *Macromolecules* 32 (1999) 375–380, <https://doi.org/10.1021/ma9814548>.
- [108] L.M. Robeson, Z.P. Smith, B.D. Freeman, D.R. Paul, Contributions of diffusion and solubility selectivity to the upper bound analysis for glassy gas separation membranes, *J. Membr. Sci.* 453 (2014) 71–83, <https://doi.org/10.1016/j.memsci.2013.10.066>.